Response to Reviewer Comments

We thank the editor and two reviewers for their detailed comments, which improved the quality and clarity of this manuscript.

The *italicized text* below reflects the reviewer's remarks, while our responses are presented in normal text. Blue text is used to cite passages from the revised manuscript and track the changes made. References cited in the blue text can be found in the revised manuscript. When page and line numbers are specified, they refer to the clean version of the revised manuscript.

EDITOR 1 (EC1)

Dear authors,

As the topical editor, I am guiding the review process of your article and will rely on the feedback of the independent reviewers. However, as a scientist, I am also following your work with great interest. I would like to start a discussion and get your view on the similarities and differences in the approach you followed with the CoCiPGrid modelling and the work that we were doing in setting up, what we called, climate change functions (CCF, earlier also called climate cost functions, but then renamed later due to stakeholder feedbacks). Both are Lagrangian approaches, where atmospheric (physical and chemical) processes are considered in advected air parcels and a metric on the radiation change is mapped back to the emission grid. This enables this kind of "short-cut" or parametric link between a local aviation emission and induced changes in the radiative budget over the lifetime of the considered effects with respect to the advected air parcel.

Note this should not be confused with the more simplified approach of the algorithmic climate change functions (aCCF) that constitute a statistical relation between the meteorology at time of emission and the estimated CCF value.

Hence, for the sake of clarity, there are two points that might be of interest to science and to stakeholders (e.g. airspace users):

1. *What are the similarities and differences in the modelling approaches of CoCiPGrid and CCF?*
2. *If the modelling approaches are similar, would it make sense to use one common language and name this specific modelling in a similar way?*

CCF modelling approach:

Grewe, V., Frömming, C., Matthes, S., Brinkop, S., Ponater, M., Dietmüller, S., Jöckel, P., Garny, H., Dahlmann, K., Tsati, E., Søvde, O. A., Fuglestvedt, J., Berntsen, T. K., Shine, K. P., Irvine, E. A., Champougny, T., and Hullah, P.: Aircraft routing with minimal climate impact: The REACT4C climate cost function modelling approach (V1.0), Geosci. Model Dev. 7, 175-201, doi:10.5194/gmd-7-175-2014, 2014.

CCF Modelling results:

Frömming, C., Grewe, V., Brinkop, S., Jöckel, P., Haselrud, A.S., Rosanka, S., van Manen, J., and Matthes, S., Influence of the weather situation on non-CO_2 aviation climate effects: The

REACT4C Climate Change Functions, Atmos. Chem. Phys. 21, 9151-9172, https://doi.org/10.5194/acp-21-9151-2021, 2021.

Final remark:

Note that due to my role as topical editor this comment will not influence any decision on a potential acceptance of the publication.

Volker Grewe

- Thank you for this feedback and suggestion. We should have included the these papers in the original manuscript, which are highly relevant. Here, we compare the similarities and differences between the grid-based CoCiP and climate change functions (CCF), focusing specifically only on contrail modelling.
- We have identified the several similarities between the grid-based CoCiP and CCFs:
    i. Both approaches use a Lagrangian framework and parameterised physics to simulate contrails,
    ii. Both simulate the contrail climate forcing throughout their full lifecycle and attribute these effects back to the original grid cell, and
    iii. Both produce a map of regions forecast with warming and cooling contrails, subsequently using it as a cost function for optimising flight trajectories.
- The main differences between the grid-based CoCiP and CCFs are as follows:
    i. The grid-based CoCiP uses reanalysis and forecast data, while CCFs rely on representative weather patterns in the North Atlantic,
    ii. CCFs include second-order effects, such as contrail-atmosphere humidity exchange, changes in temperature lapse rate, and changes in natural cirrus occurrence and properties, all of which are not accounted for in the grid-based CoCiP which runs in an offline mode, and
    iii. CCFs can compute the effective radiative forcing and surface temperature effects, while the grid-based CoCiP only calculates the instantaneous radiative forcing, and
    iv. The grid-based CoCiP includes different aircraft-engine groups, accounting for variations in aircraft mass, overall efficiency, and nvPM number emissions, which can affect the simulated contrail properties as supported by measurements and observations (Gryspeerdt et al., 2024; Jeßberger et al., 2013; Märkl et al., 2024), whereas nvPM effects are not captured in the CCF.
- In summary, both approaches have their strengths and limitations and are suited to different purposes. For example, CCFs may provide a more accurate representation of the contrail climate effects than the grid-based CoCiP, as they account for atmospheric interactions and second-order effects. However, this comes at the expense of significantly greater computational demands, where CCFs require approximately 3.3 CPU hours to compute the aviation-induced climate effects per grid cell and per time slice, as estimated from Section 2.5 of Frömming et al. (2021). The grid-based CoCiP takes around 10 CPU minutes to compute the global 3D $EF_{contrail}$ ($0.25° \times 0.25° \times 18$ pressure levels) for each time slice. The large computational demands of CCFs

potentially reduces their viability for real-time flight trajectory optimization, unless it is applied in the form of algorithmic climate change functions (aCCF). Additionally, the lower spatiotemporal resolution of the CCFs (168 grid points × 3 emission times) compared to the grid-based CoCiP, which uses ERA5 meteorology (0.25° longitude × 0.25° latitude × 18 pressure levels × 1 h) in our implementation in this manuscript, may limit the CCF's ability to accurately capture the structure and location of ice supersaturated regions (Wolf et al., 2024). Nevertheless, it should also be noted that the spatiotemporal resolution of the ERA5 HRES is also not high enough to fully address these limitations.

- We agree that the both grid-based CoCiP and CCFs aim to quantify the contrail climate effects, albeit using different metrics ($EF_{contrail}$ versus ATR, AGTP, and AGWP). However, we have decided against using a common naming convention to delineate the differences between the instantaneous radiative effects and longer feedbacks. While we can roughly convert $EF_{contrail}$ to other climate metrics that can account for second-order and longer-term climate feedback, we aim to create a stronger link between the computationally efficient $EF_{contrail}$ calculation and the more rigorous CCF calculations in future work. This has now been mentioned in the conclusions. We have made the following changes in the revised manuscript to incorporate these comments:
    - [Main text: Lines 50 – 58] "~~To simulate the full contrail lifecycle and climate forcing, earlier studies have relied on~~ **Various** physics-based modelling approaches **have been employed for this purpose**, including**: (i)** large-eddy simulations (LES) (Lewellen, 2014; Lewellen et al., 2014; Unterstrasser, 2016)**; (ii)** ~~and~~ parameterised Lagrangian models such as the Contrail Cirrus Prediction Model (CoCiP) (Schumann, 2012), Contrail Evolution and Radiation Model (CERM) (Caiazzo et al., 2017), and Aircraft Plume Chemistry, Emissions, and Microphysics Model (APCEMM) (Fritz et al., 2020)**; and (iii)** ~~. Contrails have also been parameterized in~~ general circulation models (GCMs) **which simulate the interactions between contrails and different atmospheric** ~~to capture the physical~~ processes ~~of the atmosphere and longer-range spatiotemporal,~~ **including second-order** feedback **mechanisms** (Bier and Burkhardt, 2022; Chen and Gettelman, 2013; **Grewe et al. 2014;** Ponater et al., 2021). **Specifically, approaches (ii) and (iii) have been applied to investigate the spatiotemporal variations in contrail climate effects and used for flight trajectory optimisation purposes (Frömming et al., 2021; Grewe et al., 2017; Schumann et al., 2011; Teoh et al., 2020b).**"
    - [Main text: Lines 86 – 89] "~~The~~ **Our** contrail forecasting **tool uses** ~~strategy is based in~~ a Lagrangian model instead of LES and GCMs **for two key reasons: (i)** ~~because~~ it can **utilise** ~~most efficiently compute the $EF_{contrail}$ using~~ reanalysis or forecast meteorolog**ical~~y~~ data** provided by numerical weather prediction (NWP) models**, rather than relying on representative weather conditions from GCMs (Grewe et al., 2014); and (ii) it can compute the $EF_{contrail}$ efficiently within the time constraints required for flight planning and operational use**."
    - [Main text: Lines 527 – 535] "To implement this mitigation strategy in the real-world, we developed a tool that **uses reanalysis or forecast meteorology to** generate~~s~~ global maps **of** ~~forecasting regions with~~ persistent contrail~~s and their~~ **climate forcing within the timeframe necessary for flight planning and**

operational deployment. This is achieved by extending the existing trajectory-based CoCiP, which simulates contrails formed along flight trajectories, to a grid-based approach, which initializes an infinitesimal contrail segment at every point in a spatiotemporal grid and simulates the contrail climate forcing over its lifecycle. The model outputs of the grid-based CoCiP (i.e., the 5D $EF_{contrail}$ per flight distance with dimensions of longitude × latitude × altitude × time × N aircraft-engine groups) are **similar to the concept of climate change functions (CCF) introduced in previous studies (Frömming et al., 2021; Grewe et al., 2014), and** provided in a format that is consistent with standard weather and turbulence forecasts so it can be readily integrated into existing flight planning software."

- [Main text: Lines 537 – 544] "Our comparison of the $EF_{contrail}$ estimates between the grid-based and trajectory-based CoCiP demonstrates a good agreement for use as a prototype contrail forecasting tool (Table 4). When the grid-based CoCiP is configured with $N \geq 7$, the mean error across all performance metrics is up to 3% when compared with the configuration without any aircraft-engine grouping. Alternatively, a configuration of $N = 3$ for the grid-based CoCiP provides operational simplicity for end users, but this comes at an expense of increasing the mean error across all metrics to 13%. **While the model simplifications required for the grid-based CoCiP inevitably lead to additional uncertainties in the absolute $EF_{contrail}$ values, we consider their relative spatiotemporal variabilities to be more relevant for the study's objective of identifying regions with strongly warming contrails (i.e., $EF_{contrail} > 80^{th}$ or 95^{th} percentile) for flight trajectory optimisation (Grewe et al., 2014).**"
- [Main text: Lines 557 – 562] "We acknowledge that the widespread adoption of our contrail forecasting tool in real-world operations depends on a successful validation of its predictions against independent observations. The ongoing focus on observational validation for both CoCiP variants underscores the active efforts in this critical area. **While multiplying the $EF_{contrail}$ by the ERF/RF ratio, c.f., Eq. (8), was used in this study to provide a highly approximate estimate of second-order and longer-term climate feedback, our future work aims to establish a stronger connection between this computationally efficient $EF_{contrail}$ calculation and the more rigorous CCF calculations (Frömming et al., 2021).**"

REFEREE 1 (RC1)

General comments

The authors describe the implementation of a new tool for contrail-avoiding flight-routing that is aimed at producing forecasts of fields of the so-called Energy Forcing (EF), similar in format to other fields of standard weather maps. These fields can then be used for flight-routing that optimizes flight tracks in a way that the total path-integrated EF is minimal. I am pleased that the authors see the necessity to test their predictions thoroughly with independent data and to investigate the sensitivity to uncertain parameters of their approach. Thus, this development is on a good way and the description of the code fits well to GMD. However, I have two major reservations to the current approach, which should be addressed in the final paper.

Major comments

1. *All the results that this method produces and will produce and many results that are cited are based on the "parametric RF model" by Schumann et al. (2012). This "model" is not a model but a fit to results from 1000s radiative transfer calculations using a large set of profiles as input. It must be recognized that a fit is not a model. I suggest to search the internet for "fit vs. regression". What would be required for the current purpose is a regression rather than a fit. The fit that is used so far has more than 10 free parameters. It is quite possible that this leads to overfitting (that is, fitting of noise). Testing of the fit against independent test profiles has never been performed, as far as I know. Thus it is unknown whether there is overfitting or not. Moreover, there is to my knowledge no analysis of the residuals, whether they are distributed homogeneously or not over the range of input variables. Thus, it is in particular not known, how the fit behaves under conditions that lead to the strongest warming. There are often statements that 2-3% of contrails contribute 80% of the overall EF, but whether this statement is tenable cannot be judged without an analysis of the residuals.*

   I do not expect that the "RF model" will be thoroughly tested for the current paper, but these tests should certainly by placed on the agenda for the near future. For the present paper I expect to see a section in the discussion where these issues are discussed and I expect that statements that are based on results of this RF model are turned moderate.

   - Thank you for this feedback. We have decided to retain the term "parametric RF model" in the revised manuscript to remain consistent with Schumann et al. (2012) while clarifying that this model is indeed a fit to the libRadtran radiative transfer package. Additionally, we have also included a discussion on the sensitivity of $EF_{contrail}$ to various factors and emphasise that both contrail lifetime and RF influence the $EF_{contrail}$ estimates.
   - We acknowledge your concerns about potential overfitting and the lack of testing against independent profiles. These issues can be captured within the Monte Carlo simulation framework, for example, using the approach of a recent study which evaluated the $EF_{contrail}$ uncertainties resulting from the parametric RF model and other sources (meteorology, emissions, and model parameter uncertainties) (Platt et al., 2024). We have noted this approach as part of the future roadmap to improve the grid-based CoCiP (see Lines 256 – 257 and 562 – 563 of the revised manuscript).
   - Finally, we have adjusted the $EF_{contrail}$ values in the revised manuscript, reducing the precision from three to two significant figures, to better reflect the underlying uncertainties.
   - The following changes has been made in the revised manuscript:
     - [Main text: Lines 121 – 123] "A~~t each time step, a~~ parametric RF model**, which is fitted to the libRadtran radiative transfer package (Mayer and Kylling, 2005), is used to** estimate~~s~~ the local contrail SW and LW RF (RF', the change in radiative flux over the contrail coverage area) **at each time step** (Schumann et al., 2012a)~~,~~**.**"

- [Main text: Lines 129 – 142] "The $EF_{contrail}$ is estimated by **integrating the** ~~multiplying~~ local contrail net RF' **over** ~~by~~ its contrail segment length (L)**,** ~~and~~ width (W)**,** and ~~integrated over its~~ lifetime (t_{max}) (Schumann et al., 2011),

$$EF_{contrail}\ [J] = \int_0^{t_{max}} RF'_{net}(t) \times L(t) \times W(t)\ dt. \quad (4)$$

~~The estimated RF'_{net} and $EF_{contrail}$ account for the presence of natural cirrus above/below the contrail (Schumann et al., 2012), and recent CoCiP studies have further formulated an approach to approximate the change in contrail RF'_{net} due to contrail-contrail overlapping (Schumann et al., 2021; Teoh et al., 2024a). For this study, w~~**W**e note that the $EF_{contrail}$ is ~~contrail diffusivity, ice crystal loss rate, lifetime, and climate forcing are~~ sensitive to **several factors, including the: (i) contrail RF' estimates from the fitted parametric RF model; (ii) humidity fields from the NWP model, which affects the contrail t_{max} and coverage area (L and W); and (iii)** ~~the~~ contrail segment angle (α), **which is** the angle between the contrail segment and the longitudinal axis~~)~~. **For (iii),** ~~because~~ α influences the magnitude of wind shear acting **perpendicular** ~~normal~~ to the contrail segment ($\frac{dS_n}{dZ}$) (Schumann, 2012),

$$\frac{dS_n}{dZ} = \frac{dV}{dZ}\cos(\alpha) - \frac{dU}{dZ}\sin(\alpha), \quad (5)$$

where $\frac{dV}{dZ}$ and $\frac{dU}{dZ}$ **represent** ~~are~~ the ~~magnitude of~~ wind shear acting on the eastward and northward direction respectively. **The $\frac{dS_n}{dZ}$, in turn, influences the contrail's spreading rate, ice crystal loss rate, and t_{max}. Consequently, contrails with a large $EF_{contrail}$ are generally long-lived with a large coverage area, while short-lived contrails with a large positive net RF' may have a negligible $EF_{contrail}$ (Teoh et al. 2020a).**"

- [Main text: Lines 250 – 257] "**We note that the uncertainties in the simulated $EF_{contrail}$ can arise from multiple independent sources, including meteorological inputs provided by NWP models, aircraft performance and emissions estimates, contrail model simplifications, the parametric RF model fitted to the libRadtran radiative transfer package, and potentially other unidentified factors (Low et al., 2024; Platt et al., 2024; Schumann et al., 2021; Teoh et al., 2020b, 2024a). While Platt et al. (2024) evaluates various uncertainty sources affecting $EF_{contrail}$ in an earlier implementation of the grid-based CoCiP, the Monte Carlo simulations in this study focus only on uncertainties related to meteorological inputs and the grid-based model simplifications (i.e., aircraft-engine groups and the treatment of α) as a proof of concept. Future updates to the grid-based CoCiP will incorporate additional uncertainty sources to improve the model's robustness.** "
- [Main text: Lines 562 – 563] "Future versions of the grid-based CoCiP are also expected to be prioritised towards: (i) accounting for **different** ~~contrail model~~ uncertaint**yies** **sources** within the ~~framework of the~~ Monte Carlo **contrail** simulation **framework** (Platt et al., 2024);"

2. *Some parts of the model are much more detailed than others. For instance, details on aircraft/engine combinations up to engine details are required as input in order to make a*

precise prediction of the emission rate of NvPMs. At the same time, the precision of the weather input is certainly much lower (vertical resolution is low, hourly output, problems with the field of relative humidity, etc.), the ERF/RF ratio can only be estimated, other quantities have a very wide 5-95% confidence interval. It seems that this combination of very precise vs quite imprecise parts may lead to funny results. I was puzzled, on page 22, that in the first paragraph some quite uncertain parameters are used while in the next paragraph results are given with a very high precision, e.g. 213,357 +- 0.03 kg. Considering, for instance, the range of social carbon cost, roughly 44 to 410 USD, I would suggest that of the 213,357 kg maybe the first digit is valid, but not more.
I would like to see what the authors think about this mixture of very detailed vs. very uncertain parts of their model.

- Detailed engine information is crucial, as the nvPM number emissions index (EI_n) can vary by up to five orders of magnitude between different aircraft-engine types. We note that the aircraft-engine grouping in the grid-based CoCiP reduces the precision of the nvPM EI_n estimates.
- Nevertheless, we acknowledge that differences in both the accuracy and precision of the different input parameters (fuel consumption, nvPM, and meteorology) would propagate to the estimated $EF_{contrail}$ from the grid-based CoCiP. To incorporate this feedback, we have rounded the reported $EF_{contrail}$ to 1–2 significant figures. Additionally, we have rounded the total CO_2 mass-equivalent estimates (including both fuel and contrail climate forcing) are rounded to the nearest tonne, rather than rounding to the first digit as suggested by the reviewer, because the accuracy of CO_2 emissions from burning fuel can be estimated to within ±10%, as indicated in an in-house analysis by comparing the aircraft performance model with flight data recorders.
- We also acknowledge the significant uncertainties in the ERF/RF ratio. By providing a range for the ERF/RF ratio, end users have the option to use the lower bound for a more conservative estimate of the contrail climate effects.
- We note that the social cost of carbon is included in the text solely to enable end users to monetise the $EF_{contrail}$ if necessary, and it is not required to calculate the CO_2 mass-equivalent emissions.
- The following changes have been made to the revised manuscript:
    - [Main text: Lines 447 – 464] "The 4D $EF_{contrail}$ per flight distance fields (shown in Fig. 4a) take the form of a standard weather forecast field and can be incorporated into the flight trajectory optimizer as an additional cost factor alongside existing cost parameters such as the fuel consumption and overflight charges (Martin Frias et al., 2024). To do so, flight planners can convert the $EF_{contrail}$ to a CO_2 mass-equivalent ($m_{CO_2\ \mathrm{eq,}\mathbf{contrails}}$) (Teoh et al., 2024a),

$$m_{CO_2\ \mathrm{eq,}\mathbf{contrails}}\ [\mathrm{kg}] = \frac{\mathrm{EF}_{\mathrm{contrail}} \times \left(\frac{\mathrm{ERF}}{\mathrm{RF}}\right)}{\mathrm{AGWP}_{CO_2,\mathrm{TH}} \times S_{\mathrm{Earth}}}, \quad (8)$$

      where the **global mean** ERF/RF ratio of 0.42 **is used** ~~applied~~ as a best estimate ~~value~~ to convert the RF to an ERF estimate (Lee et al., 2021). **Given the significant uncertainties in the global mean ERF/RF ratio (ranging from**

0.21 to 0.59, based on four global climate model studies) (Bickel, 2023; Bickel et al., 2019; Ponater et al., 2005; Rap et al., 2010) and its spatiotemporal variabilities, flight planners can choose the lower bound to conservatively incorporate the contrail climate effects. $AGWP_{CO_2,TH}$ is the CO_2 absolute global warming potential over a selected time horizon (TH) (7.54 $\times 10^{-7}$ J m^{-2} per kg-CO_2 for 20 years, or 2.78 $\times 10^{-6}$ J m^{-2} per kg-CO_2 for 100 years) (Gaillot et al., 2023), and S_{Earth} is the Earth surface area (5.101 $\times 10^{14}$ m^2). If necessary, the $m_{CO_2,eq}$ can be further converted to a monetary value by multiplying it with the social cost of carbon (SC_{CO_2}), which **we assume to be** ~~is around~~ US$ 185 [US$ 44 – 413, 5–95% range] per tonne of CO_2 (Rennert et al., 2022). Here, we apply Eq. (8) in the ~~flight~~ trajectory optimizer to minimise the total CO_2 **mass-equivalent** emissions ($m_{CO_2,total} = m_{CO_2,fuel} + m_{CO_2,eq}$)**,** ~~and~~ assum**inge** a 100-year time horizon for the CO_2 AGWP**, and rounding the results to the nearest tonne to align with the precision of the input parameters**. We note that this is only one example of cost function, and that many other metrics are possible. The task of defining an appropriate cost function to assess trade-offs between contrail and CO_2 climate forcing remains a critically important topic for future research."

- [Main text: Lines 466 – 472] "Using this cost-based approach, the flight trajectory optimizer successfully lowered the $m_{CO_2\ eq,total}$ by 64%, from 597~~,198~~ **tonnes** ~~kg~~ (203~~,285~~ **tonnes** ~~kg~~ of CO_2 emitted from the total fuel consumed + **394**~~393,913~~ **tonnes** ~~kg~~ from contrails) in the original trajectory to 213~~,357~~ **tonnes** ~~kg~~ (213~~,357~~ **tonnes** ~~kg~~ + 0~~.03 kg~~ **tonne**) in the optimized trajectory. In simpler terms, more than 99.9% of the total $EF_{contrail}$ (1.3~~3~~ $\times 10^{15}$ J in the original trajectory vs. 1.0~~4~~ $\times 10^{8}$ J in the optimized trajectory) is mitigated at the expense of a **5**~~4.7~~% increase in total fuel consumption. This is achieved by: (i) lowering the cruise altitude from 36,000 to 30,000 feet between 02:45 and 05:00 UTC; followed by (ii) a further descent to 28,000 feet between 05:00 UTC and 06:30 UTC to avoid regions forecasted with persistent warming contrails; and then (iii) climbing to a final cruise altitude of 40,000 feet at around 06:30 UTC ~~to minimise the fuel consumption rate~~ (Fig. 8a)."
- [Main text: Lines 481 – 486] "Using the 80th percentile contrail-avoidance polygons, the optimizer recommends a trajectory that reduces $m_{CO_2,total}$ by 60~~1~~%, from 597~~,198~~ **tonnes** ~~kg~~ (203~~,285~~ **tonnes** ~~kg~~ of CO_2 emitted from the total fuel consumed + **394** ~~393,913~~ **tonnes** ~~kg~~ from contrails) in the original trajectory to **236** ~~235,782~~ **tonnes** ~~kg~~ (207~~,379~~ **tonnes** ~~kg~~ + 28~~,403~~ **tonnes** ~~kg~~) in the optimized trajectory. Put differently, 93% of the total $EF_{contrail}$ (1.3~~3~~ $\times 10^{15}$ J in the original trajectory vs. 9.6~~59~~ $\times 10^{13}$ J in the optimized trajectory) is avoided with a fuel penalty of 2~~.0~~% ~~(Fig. 8b)~~. This approach involves lowering the cruise altitude from 36,000 to 30,000 feet between 03:00 and 05:00 UTC, followed by a step climb to 40,000 feet at 05:00 UTC to exploit a gap in the contrail-avoidance polygon **(Fig. 8b)**."

Special comments and questions

3. *General: Please be careful to distinguish between strong radiative/energy forcing vs. warming/climate impact. As contrails might have a low efficacy and as that may depend on*

location and situational circumstances (feedbacks), strong forcing and strong warming are not equivalent.

- Thank you for highlighting this important distinction. After careful consideration, we have decided to retain the term "strongly warming contrails" rather than changing it to "strongly forcing contrails", primarily because it is more intuitive for a broader audience. In contrast, "strongly forcing contrails" could imply a large positive or negative value, which may be less clear.
- However, we also recognise the need to clarify that in this study, the terms "warming/cooling" refers to the change in net energy balance at the top of the atmosphere (TOA) and the actual surface temperature change depends on the contrail efficacy and spatiotemporal factors. Therefore, we have revised the introduction to make this distinction clear:
    - [Main text: Lines 60 – 66] "Recently, Teoh et al. (2024a) used CoCiP to simulate contrails globally for 2019, estimating that around 20% of all flights produced persistent contrails. Among these persistent contrail-forming flights, 70% of them (17% of all flights) had a net warming effect and 10% of them (2.7% of all flights) were responsible for 80% of the global annual contrail energy forcing ($EF_{contrail}$~~;~~**).** ~~i.e., t~~**The** $\mathbf{EF_{contrail}}$ **represents** the cumulative contrail climate forcing over its lifetime**, with a positive value indicating more energy entering the Earth system than leaving it. We use the terms "warming/cooling" effect to describe this net energy balance at the top of the atmosphere, while acknowledging that the actual surface temperature change depends on the contrail efficacy and spatiotemporal factors (Bickel et al., 2019; Ponater et al., 2005, 2021; Schumann and Mayer, 2017)**."

4. *L 42: Isn't a negative exponential distribution simply an exponential distribution?*
    - Thank you for highlighting this. We initially used the term "negative exponential distribution" to emphasize that the distribution declines as contrail age increases. However, upon further investigation, we agree that the terms "exponential distribution" is the correct term and refers to the same concept. We have revised this sentence accordingly:
        - [Main text: Lines 39 – 40] "These persistent contrails exhibit lifetimes that generally follow a**n** ~~negative~~ exponential distribution with a mean duration of 1–3 h (Caiazzo et al., 2017; Teoh et al., 2024a; Vázquez-Navarro et al., 2015)."

5. *L 44: What exactly is meant with the word "localised"?*
    - Thank you for pointing this out. In the context, we used the word "localised" warming effect to refer to the immediate warming effect of persistent contrails on the surrounding air, as opposed to the delayed warming effect on the Earth's surface. However, we realise that this distinction may not be necessary and have decided to remove the word "localised" to prevent confusion:
        - [Main text: Lines 40 – 43] "**During daylight hours, persistent contrails can cause a cooling effect by reflecting incoming shortwave (SW) solar radiation back to space. However, they** ~~Persistent contrails~~ always induce a

~~localised~~ warming effect by absorbing and re-emitting outgoing longwave (LW) infrared radiation~~. They can also cause a cooling effect during daylight hours by reflecting incoming shortwave (SW) solar radiation back to space~~ (Meerkötter et al., 1999).”

6. *L 50ff: The sentence is a bit misleading. Both satellite images and ground based cameras cannot only observe contrail formation, they see old contrails as well when they move through the field of view. That one is currently not able to integrate RF over a contrail's lifetime, is another - independent - issue. Perhaps it is just infeasible for long-living contrails, but in principle it seems possible to me. I have also problems to see the connection between this sentence and the remaining ones in this paragraph.*

   - Thank you. We agree with this feedback and have revised this paragraph to clarify that: (i) satellites and ground-based cameras can observe both contrail formation and evolution; and (ii) the only approach currently available to estimate the cumulative contrail climate forcing is through simulation-based estimates:
     - [Main text: Lines 47 – 50] “**While** ~~O~~**o**bservational tools such as satellite imagery and ground-based cameras **have been used for observing** ~~offer the means to monitor~~ contrail formation and ~~early~~ evolution (Duda et al., 2019; Mannstein et al., 2010; Rosenow et al., 2023; Schumann et al., 2013b; Vázquez-Navarro et al., 2015), **estimates of the cumulative contrail climate forcing over their entire lifecycle are currently only available through simulation-based models.** ~~but they are currently unable to determine the RF over a contrail’s lifetime.~~”

7. *L 66 ff: The first contrail avoidance trial was the MUAC/DLR trial, not the American Airlines trial. Moreover, the MUAC/DLR trial is, as far as I am aware of, the only one that was thorougly analysed and the experiment and analysis is published in a peer-reviewd paper by Sausen et al. (Can we successfully avoid persistent contrails by small altitude adjustments of flights in the real world? Meteorol. Z., 33(1), 83-98. 10.1127/metz/2023/1157). This paper instead of the grey literature should be cited here. If you know of other peer-reviewed analyses of such trials, please let the reader know.*

   - Thank you for bringing this to our attention. We have replaced the previous citation (Lokman, 2022) with the peer-reviewed journal article (Sausen et al., 2023):
     - [Main text: Lines 68 – 70] “While two small-scale operational contrail avoidance trials have been conducted in recent years (American Airlines, 2023; ~~Lokman, 2022;~~ **Sausen et al., 2023**), several challenges must be addressed to implement a contrail-minimisation strategy at a larger-scale.”
   - Additionally, please note that the “Copernicus Publication” citation style lists references in alphabetical order, so the order of citations should not be interpreted as indicating the timeline of the trials.

8. *L 68 ff: I find the rest of this paragraph a bit too optimistic. It appears as when the list of current problems is quite short and that they are easily solvable by selecting a certain kind of format for model output.*

- Thank you for this feedback. We have revised the manuscript accordingly:
    - [Main text: Lines 70 – 78] "**These** ~~Such~~ challenges include ~~the~~: (i) integrati**ng**~~on of~~ a contrail forecast model into flight planning and management software to **account for airspace and operational constraints** ~~optimize flight trajectories~~; (ii) automati**ng**~~on of operational~~ **airspace** procedures to perform trajectory adjustments**, which is necessary to reduce air traffic controller workload** (~~Lokman, 2022;~~ Molloy et al., 2022**; Sausen et al., 2023**); ~~and~~ (iii) **incorporating** ~~inclusion of~~ meteorological and contrail forecast uncertainties in**to** the decision-making framework for contrail mitigation actions (Agarwal et al., 2022; Gierens et al., 2020; Molloy et al., 2022)**; and (iv) balancing trade-offs between reducing contrail climate forcing and potential increases in fuel consumption**. ~~All three c~~**C**hallenges **(i) to (iii) could** ~~can effectively~~ be addressed **by providing** ~~if the~~ contrail climate forcing forecasts ~~can be provided~~ in a format similar to turbulence forecasts (Turbli, 2024), **thereby facilitating their integration** ~~so that they can be readily integrated~~ into the operational workflow of existing flight planning software (Martin Frias et al., 2024)."

9. *Figure 3: Please explain the strange structures around x,y=+-10(-7).*

- The axes in this figure use a logarithmic scale for $|EF_{contrail}| > 10^7$ J m^{-1} and a linear scale between 10^{-7} and 10^7 J m^{-1}. To address this comment, we have updated the figure caption to clarify that the box-like structures around 10^{-7} and 10^7 J m^{-1} result from the transition between the linear and logarithmic scales:

    - [Main text: Lines 303 – 307] "Figure 3: Pointwise errors between $EF^{traj}_{contrail}$ and $EF^{grid}_{contrail}$ when the grid-based CoCiP is configured: (a) using the exact/original aircraft-engine types (i.e., the same as the trajectory-based CoCiP); and with (b) N=7; (c) N=3; and (d) N=1 aircraft-engine groups respectively. Each panel contains 10,000,000 randomly-sampled flight waypoints. The axes use a logarithmic scale for $|EF_{contrail}| > 10^7$ J m^{-1} and a linear scale between 10^{-7} and 10^7 J m^{-1}. **For both axes, the box-like structures observed around 10^{-7} and 10^7 J m^{-1} arise from the transition between the linear and logarithmic scale.**"

10. *L 365 ff: Please reformulate this sentence "The 2019 ...". It is not clear what you mean.*

- Thank you for highlighting this. We have revised this paragraph for clarity improvements:

    - [Main text: Lines 389 – 396] "Unlike a map of the ISSR coverage area, which identifies regions **likely** ~~prone~~ to **form** persistent contrail**s** ~~formation~~, the 4D $EF_{contrail}$ per flight distance **accounts for the intensity of contrail-induced warming and allows for more** ~~estimates the expected contrail climate forcing of flying through a specific airspace. This approach enables~~ targeted mitigation**. For example, in 2019, the** ~~by identifying regions forecast to produce strongly warming contrails (i.e., grid cells with $EF_{contrail}$ greater than the 80th percentile), rather than all persistent contrails. When considering navigational contrail avoidance, this approach minimises potential disruptions to air traffic management and airspace capacity. The 2019~~ global annual mean percentage

of airspace volumes forecasted with strongly warming contrails **was~~, i.e.,~~** 0.44% for $EF_{contrail}$ > **95th percentile (**1.54 ×10^{9} J m^{-1} **~~(95th percentile~~**), **and** 1.6% for $EF_{contrail}$ > **80th percentile (**5.0 ×10^{8} J m^{-1} **~~(80th percentile~~**)**. These values are up to 91% smaller than the airspace volumes with net warming contrails (~~, and~~** 4.8% for $EF_{contrail}$ > 0 **~~(net warming contrails~~**), **and ~~are~~** up to 93% smaller than the ISSR coverage area (6.6%, for $EF_{contrail} \neq 0$) (Fig. 5a). **Thus, using this approach to navigational contrail avoidance could minimise potential disruptions to air traffic management and airspace capacity, as it focuses only on the most warming contrails rather than avoiding all persistent contrails.**"

11. *L 386 ff: It is counterintuitive that areas with high cirrus coverage lead to strongly warming contrails. Please explain.*

- We have revised this paragraph to explain how regions with high albedo, which includes areas with high natural cirrus coverage, can increase the likelihood of strongly warming contrails:
    - [Main text: Lines 416 – 423] "Background radiation fields, such as the solar direct radiation (SDR), ~~reflected solar radiation (~~RSR~~)~~, ~~outgoing longwave radiation (~~OLR~~)~~ and albedo (RSR/SDR), are **mainly** influenced by latitude, natural cirrus occurrence, and surface temperature and **reflectance** ~~albedo~~. In general, **strongly warming contrails are more likely in** regions with**: (i)** ~~a~~ high~~er relative~~ albedo (e.g., poles, Siberia, and areas with high natural cirrus coverage)~~,~~**;; (ii) high** OLR (e.g., tropics and the Sahara Desert)~~,~~**;** and **(iii)** ~~a~~ low~~er relative~~ SDR (e.g., wintertime) ~~tend to exhibit more strongly warming contrails~~ (Fig. 6 and 7). **Condition (i) limits the contrail SW RF because a higher proportion of incoming solar radiation is already reflected without contrails, while condition (ii) drives the contrail LW RF especially in cloud free conditions.** In contrast, regions and times with a larger relative SDR-to-OLR ratio (e.g., Southeast Asia, springtime at high latitudes) are associated with ~~more~~ strongly cooling contrails (Fig. 7b, 7d, and 7f)."

12. *P 22: The precision of the quoted input and output values does not fit together, see major comment above.*

- Thank you. We have addressed this in Comment 2.

13. *L 521/22: I am pleased that the authors acknowledge this necessity and agree completely!*

- Thank you.

14. *L 636: Please try to find a combination of entries in a contingency table that results in ETS=-1. If you find one, please let the reader know.*

- Thank you for highlighting this. After further investigation, we confirm that an ETS score of -1 represents a theoretical lower bound and have revised this paragraph to clarify this point:

- [Main text: Lines 709 – 713] "The ERA5-corrected RHi from both methodologies (i.e., global humidity correction and quantile mapping) were compared against in-situ RHi measurements from the mid-latitude region (30°N – 70°N and 125°W – 145°E) (Hofer et al., 2024). These comparisons ~~were conducted~~ us**eding** the equitable threat score (ETS) metric, where an ETS **score of =** 1 **represents** ~~suggests~~ a perfect agreement between the ERA5-corrected and in-situ RHi **measurements**, an ETS **score of =** 0 suggests a random **agreement** ~~relationship~~, and an ETS **score below 0 signifies** ~~= -1 suggests~~ an inverse relationship."

REFEREE 2 (RC2)

General comments

This study describes a gridded version of the Contrail Cirrus Prediction model and illustrates how it could be used in various applications, including aircraft rerouting for contrail avoidance.

The paper is very well written and presents several important findings for contrail avoidance. Using Cocip to compute a grid of cumulative contrail energy forcing per flown distance is a simple and clever idea. The Monte-Carlo framework for calculating uncertainties is very welcome, because the lack of uncertainty propagation in Cocip is a strong limitation of the original model. The comparison between Cocip and CocipGrid is important to inform a potential operational use of the latter. The examples of CocipGrid-based contrail avoidance are informative illustrations. I have installed and tried CocipGrid and it was straightforward – congratulations to the developers.

Yet, there are aspects of the study that require improvement. Like much of Cocip literature, the paper does not discuss the impact of the choice of model timestep. That discussion needs to happen now, since it has direct implications for the avoidance examples given in section 5. The comparison between Cocip and CocipGrid also needs to be deepened, because the differences are large. For those reasons, and to also address the other comments below, I recommend major revisions.

Major comments

15. *Line 116: Cocip timestepping has received little attention in the literature. This study uses a timestep of 300 s (5 min), following Teoh et al. (2023). Schumann (2012) used much longer timesteps but noted that some aspects of the model are timestep-dependent (their section 2.9), unfortunately without discussing the impact on simulated contrail energy forcing. So, I ran CocipGrid on ERA5 data for the case shown in Fig 5, 7 Jan 2019 at 3am, focusing on the North Atlantic at 200 hPa. With a 5-min timestep (dt_integration parameter), I get a domain-averaged energy forcing of 6.7 10^7 J km^{-1} and a maximum of 4.8×10^9 J km^{-1}. Increasing the timestep to 15 min, the numbers become 6.4×10^7 and 4.1×10^9 J km^{-1}, respectively. At 30 min, we are down to 6.1×10^7 and 3.8×10^9 J km^{-1}. So simply changing the integration timestep decreases the domain average by almost 10% and maximum energy forcing by more than 20%. If CocipGrid is to become the basis for contrail avoidance, that needs to be addressed – otherwise actors will use whichever timestep gives the most convenient answer. Why such a large impact? Can that impact be*

reduced with further developments? If not, what guidance can be given for choosing the timestep? Are there other unexplored parameters with similarly dramatic impacts on simulated energy forcing?

- We commend the reviewer's effort in personally running the grid-based CoCiP to evaluate the sensitivity of the contrail energy forcing ($EF_{contrail}$) to the selected model time step (d*t*). In response to this comment, we have added a new section to the Appendix, which includes:
    - A discussion on the choice and rationale behind the d*t* values used in previous studies that simulated contrails with CoCiP,
    - A sensitivity analysis evaluating the impact of different d*t* values on the simulated $EF_{contrail}$ from the grid-based CoCiP, along with a short discussion on the factors causing the $EF_{contrail}$ to increase with smaller d*t* values, and
    - The rationale of selecting a d*t* of 300 s for this study, and
    - An assessment of how the choice of d*t* changes the forecast of the grid-based CoCiP, specifically regarding regions forecasted with strongly warming contrails.
- The following changes have been made to the revised manuscript:
    - [Main text: Lines 155 – 160] "We achieve this by extending the trajectory-based CoCiP to a grid-based approach, where an infinitesimal contrail segment is: (i) initialized at each point in a 4D spatiotemporal domain; (ii) simulated until its end of life with a d*t* of 300 s using the equations of the trajectory-based CoCiP; and (iii) has its cumulative climate forcing attributed back to the grid cell where it originally formed**, with the model outputs**~~. The output from this approach~~ tak**inge**~~s~~ the same form as traditional 4D NWP data. **For (ii), Appendix A2 evaluates the sensitivity of d*t* on the simulated $EF_{contrail}$ and provides the rationale for selecting a d*t* of 300 s for the grid-based CoCiP.**"
    - [Main text: Lines 488 – 495] "Figure 9: Application of the simulated $EF_{contrail}$ per flight distance for contrail mitigation ~~purposes~~, where flight planners can: (a) construct polygons and avoid flying in regions forecast with strongly warming contrails (i.e., grid cells where the $EF_{contrail}$ per flight distance is greater than the 80th percentile (5.0 ×10^{8} J m^{-1}); and/or (b) account for uncertainties in the simulated contrail climate forcing by masking and disregarding grid cells (shown in white) when their probability of forming net warming (or cooling) contrails is less than 90%. The global contrail climate forcing shown here are from the nominal nvPM aircraft-engine group and simulated at FL360 (10,973 m) on the 7th of January 2019 at 03:00:00. **For panel (a), the impact of d*t* on regions forecast with strongly warming contrails are evaluated in Appendix A2.** Basemap plotted using Cartopy 0.22.0 and sourced from Natural Earth; licensed under public domain."
    - [Appendix: Lines 648 – 683] "

      A2 Sensitivity of contrail climate forcing to CoCiP model time step

      Previous studies that simulated contrails with CoCiP have used different model time steps (d*t*) ranging between 5 and 60 minutes, depending on their specific application and available computational resources:

- Schumann et al. (2015) used a 60-minute d*t* due to: (i) CoCiP's coupling with the Community Atmosphere Model (CAM), which operates on a 60-minute time step; and (ii) the extensive computational demands of the 20-year global simulations,
- Regional studies over Japan, Europe, and the North Atlantic used a 30-minute d*t*, as these simulations were conducted locally on consumer-grade hardware (Schumann et al., 2021; Teoh et al., 2020b, 2022a),
- Schumann & Graf (2013) used a 15-minute d*t* to match the time resolution of their air traffic and satellite datasets, and
- Teoh et al. (2024a) used a 5-minute d*t* because the simulation was conducted on the cloud where computational resources were no longer constrained.

In this section, we perform a sensitivity analysis by running the grid-based CoCiP with different d*t* values of 1, 5, 10, 15 and 30 minutes and quantify their impact on the estimated $EF_{contrail}$. We specifically simulated contrails on the 7th of January 2019 at 03:00:00 UTC to be consistent with time period used in the examples in Section 5. Figure A3 shows that the simulated $EF_{contrail}$ tends to increase as d*t* decreases, with the mean $EF_{contrail}$ per flight distance simulated from a 1-minute d*t* being approximately 24% larger than those simulated from a 30-minute d*t*. The smaller $EF_{contrail}$ at larger d*t* values, such as 30-minutes, can be explained by the contrail lifetime ending prematurely. For example, if ambient conditions in the next model time step (*t* + 30 minutes) are unfavourable for contrail persistence, the $EF_{contrail}$ between t and (*t* + 30 minutes) becomes zero because contrails are no longer present at (*t* + 30 minutes). In contrast, under the same ambient conditions, a smaller d*t* of 1-minute allows the simulated contrails to persist for a longer time period within the same 30-minute window, thereby increasing the overall contrail lifetime and resulting in a larger warming or cooling effect ($|EF_{contrail}|$, as shown in the larger standard deviation in Fig. A3).

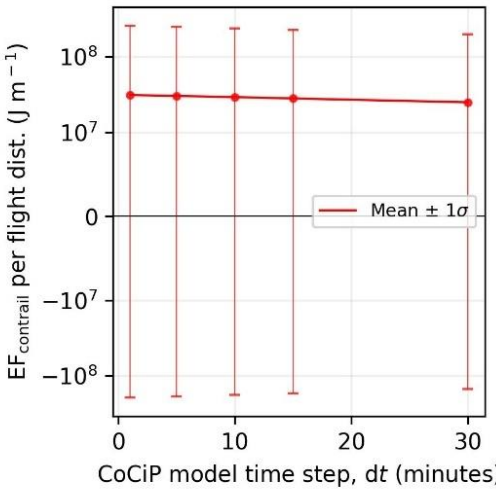

Figure A3: Change in the global mean and standard deviation of $EF_{contrail}$ per flight distance across different CoCiP model time steps (d*t*). Contrails are simulated globally at FL360 (10,973 m) on the 7th of January 2019 at 03:00:00, with the nominal nvPM aircraft-engine group. The y-axis uses a logarithmic scale for $|EF_{contrail}| > 10^7$ J m^{-1} and a linear scale between 10^{-7} and 10^7 J m^{-1}.

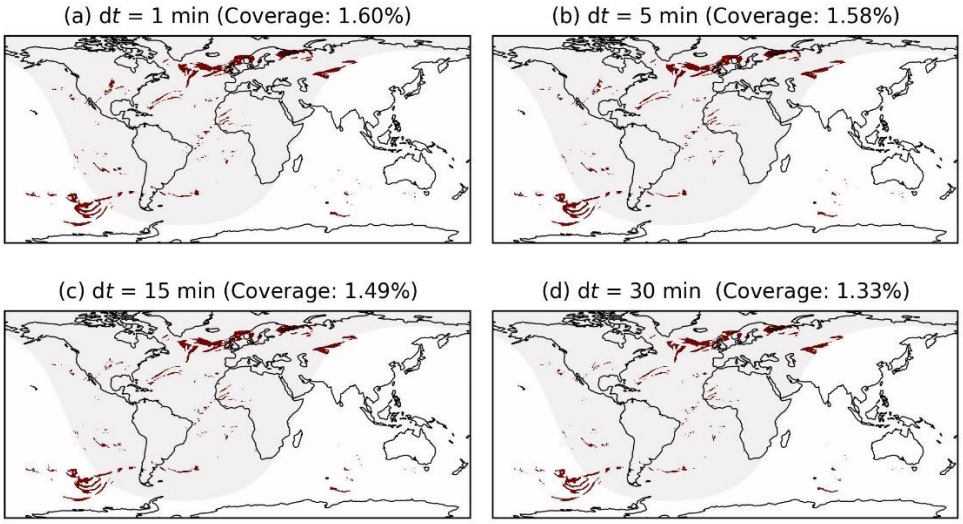

Figure A4: Regions forecasted with strongly warming contrails, i.e., $EF_{contrail}$ per flight distance > 5.0 ×10^8 J m^{-1} (80^{th} percentile) when simulated with different model time steps (d*t*) of: (a) 1-minute; (b) 5-minute; (c) 15-minute; and (d) 30-minutes. Contrails are simulated globally at FL360 (10,973 m) on the 7^{th} of January 2019 at 03:00:00, with the nominal nvPM aircraft-engine group.

In this study, we chose a 5-minute d*t* to align with Teoh et al. (2024a), as their $EF_{contrail}$ thresholds (i.e., > 80^{th} and 95^{th} percentiles) were used to identify regions that forecasted to produce strongly warming contrails. For our research objectives, we note that the choice of dt only leads to minor differences in the regions identified with strongly warming contrails (Fig. A4). While time step error is one of the many sources of errors influencing $EF_{contrail}$, our analysis shows that it is not the most dominant one especially when compared to the impact of humidity corrections applied to the ERA5 HRES (Teoh et al., 2024a)."

16. *Section 4 is very good at describing the different metrics used to compare CocipGrid to Cocip, which is a very important comparison to make, but the discussion of the results feels incomplete. Section 4.2 focuses on the impact of the choice of the number of aircraft groupings. But differences shown on Fig 3a are sizeable and raise several questions:*

    i. *What causes the differences? Is that mainly alpha and f_shear? Line 222 mentioned a calibration of f_shear. Has that been done here?*

    ii. *Many flights have zero energy forcing in either Cocip or CocipGrid when the other model has non-zero energy forcing. Why is that? Difference in contrail persistence due to different effective wind shear?*

    iii. *And why are the datapoints arranged in square patterns? Is it an artefact of the selection of comparison cases?*

- Thank you for this feedback. To address points (i) and (ii), we have now added a short discussion outlining the primary factors that contribute to the discrepancies between the trajectory-based CoCiP and the grid-based CoCiP when configured with the original aircraft-engine type for each flight:
    - [Main text: Lines 323 – 339] "Table 4 summarises the performance metrics when comparing the model agreement between the trajectory-based CoCiP and

various configurations of the grid-based CoCiP, i.e., using the original aircraft-engine type for each flight as in the trajectory-based CoCiP, and with different aircraft-engine groupings ($1 \leq N \leq 12$)~~, as outlined in Section 3 and Appendix A3~~.

~~The performance metrics f~~**F**or the original aircraft-engine group,~~ing show: (i)~~**, the** false negative and false alarm rates **are** ~~of~~ 3.2% and 10.4% respectively when evaluated against moderately warming contrails ($EF_{threshold} = 1 \times 10^7$ J m^{-1}), and 6.0% and 17.7% respectively when assessed against strongly warming contrails ($EF_{threshold} = 5 \times 10^8$ J m^{-1})**. The**~~; (ii) a~~ modified-MALE of 0.166, correspond~~sing~~ to a 47% relative error between $EF^{traj}_{contrail}$ and $EF^{grid}_{contrail}$. **These pointwise errors (shown in Fig. 3a) are independent of the aircraft-engine grouping and primarily arise from: (i) the assumption of an infinitesimal contrail segment in the grid-based CoCiP compared to a finite segment in the trajectory-based CoCiP, where the $EF^{traj}_{contrail}$ can be zero if the next flight waypoint does not form a persistent contrail; (ii) the use of nominal V_{TAS} and aircraft mass in the grid-based CoCiP, which causes differences in the downward displacement and survivability of the contrail during the wake vortex phase; and (iii) the calibrated f_{shear}, c.f. Eq. (6), which affects the $\frac{dS_n}{dZ}$, contrail diffusivity, coverage area, lifetime, and $EF_{contrail}$. For the fleet-aggregated errors, the**~~; (iii)~~ τ_w of 0.821 **demonstrates** ~~, indicating~~ a strong correlation between the rankings of $EF^{traj}_{contrail}$ and $EF^{grid}_{contrail}$**. The** ~~; (iv) a~~ change in ~~the~~ initial mitigation rate of 0.816~~,~~ suggest~~sing~~ an 18% reduction in the effectiveness of mitigating the most strongly warming contrails with the grid-based CoCiP,~~;~~ and ~~(v)~~ a change in the flight segment ratio of 1.156~~,~~ indicate~~sing~~ that interventions must be applied to an additional 16% of the total flight distance flown to mitigate 80% of the $EF_{contrail}$."

- For point (iii), the square patterns observed in Figure 3 are due to the transition from a linear scale ($EF_{contrail}$ of between 10^{-7} and 10^7 J m^{-1}) to a logarithmic scale ($|EF_{contrail}| > 10^7$ J m^{-1}). This clarification has been added to the caption of Figure 3 (see Comment 9).

Other comments

17. *Abstract: The abstract does not say anything of the differences between Cocip and CocipGrid. Those differences are not negligible and that could impact the operational use of CocipGrid, so it is important that the abstract acknowledges that fact.*

- Thank you for this suggestion. We have revised the abstract to briefly highlight the difference between the trajectory-based and grid-based CoCiP:
    - [Abstract: Lines 10 – 16] "Here, we develop a contrail forecasting tool that produces global maps of persistent contrail formation and their associated **energy** ~~climate~~ forcing **($EF_{contrail}$)**. This **is achieved by** ~~tool~~ extend**ings** the existing **trajectory-based** contrail cirrus prediction model (CoCiP)**, which simulate contrails formed along provided flight paths,** to **a grid-based approach that initialises** ~~efficiently evaluate~~ infinitesimal contrail segments ~~initialized~~ at each point in a ~~regular~~ 4D spatiotemporal grid **and tracks them** until their end-of-life. Outputs **are provided for different aircraft-engine**

groups and formatted to align with standard weather and turbulence forecasts, facilitating their ~~reported in a concise meteorology data format that~~ integrat**ione**~~s~~ **into** ~~with~~ existing flight planning and air traffic management workflows."

18. *Line 125: So Cocip does not account for the impact of underlying clouds other than cirrus? I thought it dealt with underlying cloudiness by using outgoing longwave radiation as input. Is that not the case?*

- Thank you for highlighting this. The parametric RF' model used by CoCiP indirectly incorporates the effects of natural cirrus, as their presence is captured by the reflected solar radiation (RSR), outgoing longwave radiation (OLR), and the overlying natural cirrus optical depth (τ_{cirrus}) terms (Schumann et al., 2012), all of which are provided by the ERA5 HRES. We have revised the paragraph to clarify this point:
    - [Main text: Lines 121 – 127] "~~At each time step, a~~ parametric RF model**, which is fitted to the libRadtran radiative transfer package (Mayer and Kylling, 2005), is used to** estimate~~s~~ the local contrail SW and LW RF (RF', the change in radiative flux over the contrail coverage area) **at each time step** (Schumann et al., 2012a)~~,~~**.** The**se RF'** estimate~~sd RF'$_{net}$ and EF$_{contrail}$~~ **indirectly** account for ~~the presence of~~ natural cirrus above **and** ~~/~~below the contrail **through input meteorology parameters including the reflected solar radiation (RSR), outgoing longwave radiation (OLR) and the overlying natural cirrus optical depth (τ_{cirrus})** (Schumann et al., 2012a)~~,~~**. Additionally,** ~~and~~ recent CoCiP studies have ~~further~~ formulated an approach to approximate the change in contrail **RF'** ~~RF'$_{net}$~~ due to contrail-contrail overlapping (Schumann et al., 2021; Teoh et al., 2024a)."

19. *Line 134: It would be useful to note here that "generally consistent" is a low bar, and, as acknowledged in the conclusion, a proper quantification of Cocip skill compared to observations, all the way to simulated energy forcing, remains needed.*

- Thank you for this feedback. We agree that further comparisons evaluation of CoCiP is required and have revised this sentence accordingly:
    - [Main text: Lines 144 – 147] "**While** ~~P~~previous studies **compared** ~~have shown that~~ the **distribution** ~~range~~ of simulated contrail properties from CoCiP ~~are generally consistent when compared~~ with in situ measurements, remote sensing, and satellite observations **over their lifecycle** (**Driver et al., 2024;** Jeßberger et al., 2013; **Low et al., 2024;** Schumann et al., 2017, 2021; Schumann and Heymsfield, 2017; Teoh et al., 2024a)**, further comparisons with observations remain crucial for building greater confidence in and improving the accuracy of CoCiP predictions**."

20. *Tables 2 and 3: It would be useful to have a graphical version of those Tables, showing the mass and nvPM of the individual aircraft types on a plot, to see how well separated the different aircraft groups are. Like Figure 1, but before transformation by the aircraft performance model.*

- Thank you. We agree with this suggestion and have now added the following figures (below) in Appendix A4:
    - [Main text: Lines 181 – 184] "Table 3: Summary of the aircraft properties (wingspan, service ceiling altitude, and maximum Mach number) and range of aircraft performance and emissions parameters (aircraft mass, η, and nvPM EI_n) for the 12 aircraft-engine groups. Details of the aircraft-engine types that are included in each group can be found in Table 2. **Differences in aircraft mass and nvPM EI_n among the 12 aircraft-engine groups are visualised in Fig. A5.**"
    - [Appendix: Lines 728 – 732] "Here, we propose several alternative aircraft-engine classifications with N ranging between 3 and 7 (groups) to assess the trade-offs between the model performance and computational requirements **(see Tables A1 to A5)**. **Additionally, we visualise the range of aircraft mass and nvPM EI_n for each aircraft-engine group when they are clustered into 12 groups (Fig. A5 and Table 2), 7 groups (Fig. A6 and Table A1), and 3 groups (Fig. A7 and Table A5) respectively.**"
    - [Appendix: Lines 733 – 736]

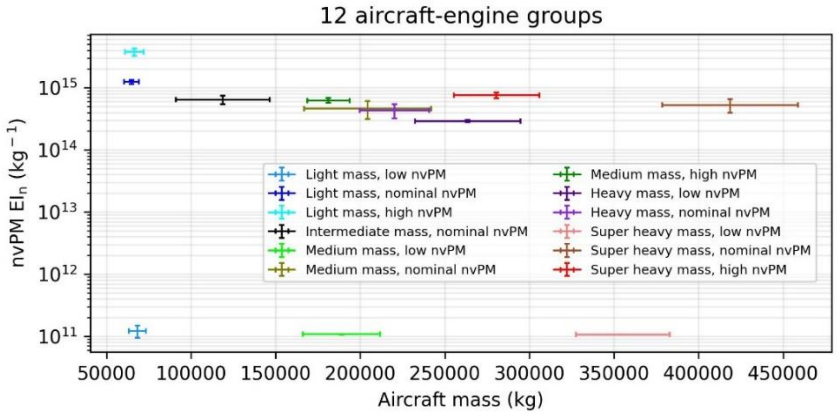

"**Figure A5: Range of aircraft mass and nvPM EI_n for each aircraft-engine group when they are clustered into 12 groups. The error bars for each data point represent one standard deviation of these values, which are provided by the 2019 global aviation emissions inventory based on ADS-B (GAIA) (Teoh et al., 2024b).**"

    - [Appendix: Lines 746 – 749]

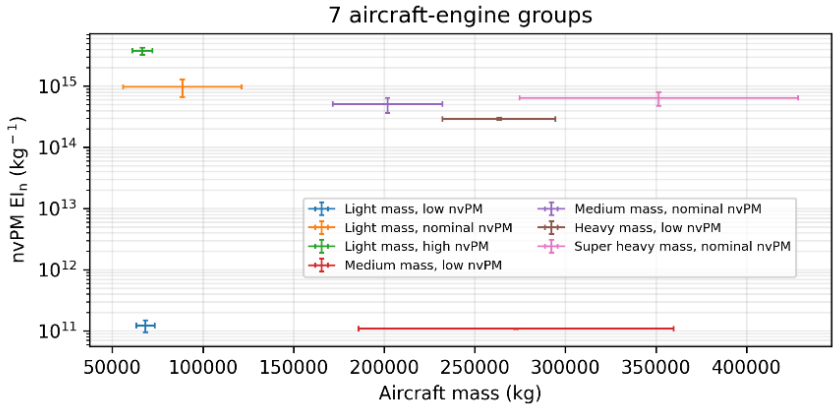

"**Figure A6: Range of aircraft mass and nvPM EI_n for each aircraft-engine group when they are clustered into 7 groups. The error bars for each data point represent one standard deviation of these values, which are provided by the 2019 global aviation emissions inventory based on ADS-B (GAIA) (Teoh et al., 2024b).**"

- [Appendix: Lines 753 – 756]

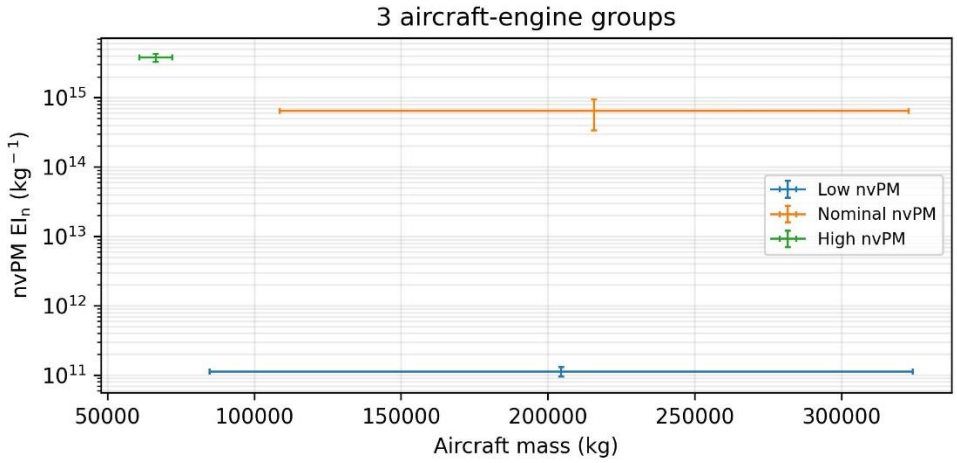

"**Figure A7: Range of aircraft mass and nvPM EI_n for each aircraft-engine group when they are clustered into 3 groups. The error bars for each data point represent one standard deviation of these values, which are provided by the 2019 global aviation emissions inventory based on ADS-B (GAIA) (Teoh et al., 2024b).**"

21. *Line 201: Could point out that the ICAO emission databank is for LTO emissions, hence the need to translate them to the more relevant cruise emissions.*

- Thank you for this suggestion. We have added a note to clarify that the ICAO emissions databank provides the nvPM emissions profile for typical engine power settings used during the landing and take-off (LTO) cycle, and the cruise nvPM EI_n is then estimated using the T_4/T_2 methodology which interpolates the LTO-based nvPM emissions profile relative to the non-dimensional engine thrust settings (Teoh et al., 2024). Additionally, we have also revised this paragraph to improve its overall flow and readability:

  - [Main text: Lines 215 – 231] "Each aircraft-engine type is characterised by a set of fixed properties, including the~~: (i)~~ wingspan**,**~~; (ii)~~ design-optimum Mach number,~~; (iii)~~ aerodynamic coefficients**,**~~;~~ and ~~(iv)~~ nvPM emissions profile, all of which are required as inputs to aircraft performance and emission models. **The** ~~Inputs (i) to (iii) are provided by the~~ Poll-Schumann (PS) aircraft performance model (Poll and Schumann, 2020, 2021) **provides the wingspan, design-optimum Mach number, and aerodynamic coefficients~~;~~,** while ~~input (iv) is provided by~~ the ICAO Aircraft Engine Emissions Databank (EASA, 2021) **supplies the nvPM EI_n at the four ICAO certification test points representing the engine power settings (i.e., 7%, 30%, 85%, and 100% of the maximum rated engine thrust) used in the landing and take-off (LTO) cycle**. For each aircraft-engine group, which encompasses multiple aircraft-

engine types (Table 2), we set these fixed properties to values of the aircraft-engine type with largest market share within the group (Teoh et al., 2024b).

~~For waypoint-specific parameters (i.e., V_{TAS}, aircraft mass, $\dot{m}_f$,, η, and nvPM EI_n), t~~**T**he nominal grid-based CoCiP **derives the waypoint-specific parameters (e.g., V_{TAS}, M, $\dot{m}_f$, η, and nvPM EI_n) using two key assumptions and two established models.** ~~obtains these parameters by~~ **Firstly, it** assum**es**~~ing~~ that the~~: (i)~~ Mach number at each grid cell is equal to the design-optimum Mach number plus 0.04 ~~to reflect real-world operational conditions~~ (Teoh et al., 2024b)**, reflecting the common practice of airlines in flying faster to minimise time-dependent costs and/or address delays (Edwards et al., 2016; Lovegren and Hansman, 2011). Secondly, it assumes that the**~~; (ii)~~ aircraft mass at each altitude is equal to the value that maximises η**, which is based on the rationale that a lower aircraft mass is required to fly at higher altitudes (Fig. 1).**~~; and using t~~**T**he ~~(iii)~~ PS ~~aircraft performance~~ model **is used** to estimate the $\dot{m}_f$ (Poll and Schumann, 2020, 2021)**, while the**~~; and (iv)~~ T_4/T_2 methodology ~~to~~ estimate**s** the nvPM EI_n **at cruise by interpolating the LTO-based nvPM emissions profile relative to the non-dimensional engine thrust settings** (EASA, 2021; Teoh et al., 2024b). ~~Assumption (i) is justified by the tendency of airlines to fly faster than the design-optimum conditions to minimise time-dependent costs and/or catch up with delays (Edwards et al., 2016; Lovegren and Hansman, 2011), while assumption (ii) is based on the rationale that a lower aircraft mass is required for the aircraft to cruise at higher altitudes (Fig. 1).~~"

22. *Line 204: Which aircraft type has the largest market share in each group? It could be good to indicate it in italics in Table 2.*

- Thank you for this suggestion. In response to this comment, we have highlighted the aircraft-engine type with the largest market share within each group in Table 2. Additionally, we also provide a quantification of the 2019 global market share for each aircraft-engine group in Table 3, based on the number of flights and the total flight distance flown.
    - [Main text: Lines 178 – 180]

Table 2: Classification of commonly used passenger aircraft-engine types into 12 unique groups based on their similarities in aircraft mass and nvPM EI_n. The aircraft types listed here are labelled based on their ICAO aircraft type designator.

Aircraft-engine classification		nvPM EI_n		
		Low	**Nominal**	**High**
Aircraft mass	**Light**	• A19N (LEAP-1A) • A20N (LEAP-1A)* • A21N (LEAP-1A) • B38M (LEAP-1B)	• A319 (CFM56) • A320 (CFM56) • A321 (CFM56) • B737 (CFM56) • B738 (CFM56)* • B739 (CFM56)	• A19N (Pratt & Whitney) • A20N (Pratt & Whitney) • A21N (Pratt & Whitney) • A319 (IAE V2500) • A320 (IAE V2500)* • A321 (IAE V2500)
	Intermediate	N/A	• B752 (RB211) • B753 (RB211) • B762 (CF6-80E) • B763 (CF6-80E)*	N/A

	Medium	• B788 (GEnx) • B789 (GEnx)***** • B78X (GEnx)	• A342 (CFM56/Trent500) • A343 (CFM56/Trent500) • A345 (CFM56/Trent500) • A346 (CFM56/Trent500) • B788 (Trent 1000) • B789 (Trent 1000)***** • B78X (Trent 1000)	• A332 (Trent 700/CF6-80E) • A333 (Trent 700/CF6-80E)*****
	Heavy	• B772 (GE90) • B773 (GE90) • B77L (GE90) • B77W (GE90)*****	• A359 (Trent XWB)***** • A35K (Trent XWB)	N/A
	Super heavy	• B748 (GEnx)*****	• A388 (Trent 900)*****	• B742 (CF6-80C) • B743 (CF6-80C) • B744 (CF6-80C)*****

***: Refers to the aircraft-engine type with the largest market share within the group, based on the 2019 GAIA dataset (Teoh et al., 2024b).**

- [Main text: Line 184]

Aircraft-engine properties and performance parameters		**nvPM EI_n**		
		Low	**Nominal**	**High**
Aircraft mass	**Light**	• Mass: 55,000 – 80,000 kg • nvPM EI_n: 1 ×10^{11} kg^{-1} • η: 0.20 – 0.26 • Wingspan: 34 – 36 m • Max altitude: 41,000 ft. • Max Mach: 0.82 • **2019 global market share** ○ **No. of flights: 1.8%** ○ **Dist. flown: 1.8%**	• Mass: 55,000 – 80,000 kg • nvPM EI_n: (0.8 – 1.0) ×10^{15} kg^{-1} • η: 0.20 – 0.26 • Wingspan: 34.1 – 34.3 m • Max altitude: 41,000 ft. • Max Mach: 0.82 • **2019 global market share** ○ **No. of flights: 37.1%** ○ **Dist. flown: 35.2%**	• Mass: 55,000 – 80,000 kg • nvPM EI_n: (2 – 4) ×10^{15} kg^{-1} • η: 0.20 – 0.26 • Wingspan: 34 – 36 m • Max altitude: 41,000 ft. • Max Mach: 0.82 • **2019 global market share** ○ **No. of flights: 12.6%** ○ **Dist. flown: 12.5%**
	Intermediate	N/A	• Mass: 85,000 – 160,000 kg • nvPM EI_n: (0.6 – 1.2) ×10^{15} kg^{-1} • η: 0.21 – 0.26 • Wingspan: 38.0 – 47.6 m • Max altitude: 43,100 ft. • Max Mach: 0.86 • **2019 global market share** ○ **No. of flights: 2.4%** ○ **Dist. flown: 4.1%**	N/A
	Medium	• Mass: 165,000 – 240,000 kg • nvPM EI_n: 1 ×10^{11} kg^{-1} • η: 0.30 – 0.34 • Wingspan: 60.1 m • Max altitude: 43,100 ft. • Max Mach: 0.90 • **2019 global market share** ○ **No. of flights: 1.0%** ○ **Dist. flown: 3.6%**	• Mass: 165,000 – 250,000 kg • nvPM EI_n: (4 – 7) ×10^{14} kg^{-1} • η: 0.29 – 0.33 • Wingspan: 60.1 – 60.3 m • Max altitude: 43,100 ft. • Max Mach: 0.86 – 0.90 • **2019 global market share** ○ **No. of flights: 0.7%** ○ **Dist. flown: 2.8%**	• Mass: 160,000 – 210,000 kg • nvPM EI_n: (0.7 – 1) ×10^{15} kg^{-1} • η: 0.25 – 0.28 • Wingspan: 60.3 m • Max altitude: 41,000 ft. • Max Mach: 0.86 • **2019 global market share** ○ **No. of flights: 2.7%** ○ **Dist. flown: 6.9%**
	Heavy	• Mass: 200,000 – 320,000 kg • nvPM EI_n: (3 – 4) ×10^{14} kg^{-1} • η: 0.28 – 0.30 • Wingspan: 64.8 m • Max altitude: 43,100 ft. • Max Mach: 0.89 • **2019 global market share** ○ **No. of flights: 1.8%** ○ **Dist. flown: 7.2%**	• Mass: 205,000 – 250,000 kg • nvPM EI_n: (5 – 8) ×10^{14} kg^{-1} • η: 0.33 – 0.35 • Wingspan: 64.7 m • Max altitude: 43,100 ft. • Max Mach: 0.89 • **2019 global market share** ○ **No. of flights: 0.5%** ○ **Dist. flown: 2.2%**	N/A
	Super heavy	• Mass: 275,000 – 400,000 kg • nvPM EI_n: 1 ×10^{11} kg^{-1} • η: 0.32 – 0.34 • Wingspan: 68.4 m • Max altitude: 42,100 ft. • Max Mach: 0.90 • **2019 global market share** ○ **No. of flights: 0.2%** ○ **Dist. flown: 0.8%**	• Mass: 385,000 – 512,000 kg • nvPM EI_n: (5 – 7) ×10^{14} kg^{-1} • η: 0.33 – 0.35 • Wingspan: 79.8 m • Max altitude: 43,100 ft. • Max Mach: 0.89 • **2019 global market share** ○ **No. of flights: 0.3%** ○ **Dist. flown: 1.6%**	• Mass: 250,000 – 360,000 kg • nvPM EI_n: (6 – 8) ×10^{14} kg^{-1} • η: 0.27 – 0.29 • Wingspan: 64.4 m • Max altitude: 45,000 ft. • Max Mach: 0.92 • **2019 global market share** ○ **No. of flights: 0.5%** ○ **Dist. flown: 1.7%**

23. *Figure 1 could do with a more detailed discussion. If I understand well, it was obtained by applying the four assumptions listed in lines 205-212 onto the input data for one aircraft group. I see that the aircraft needs to be lighter to fly higher up, which makes sense. But why are the distributions multimodal? Is that because of the different aircraft types within the group? And why does the nvPM EI distributions change with altitude? Because mass has changed?*

- Thank you for this suggestion. Figure 1 to serve two purposes in the manuscript: (i) it illustrates that a lower aircraft mass is more likely when the aircraft is cruising at higher altitudes (Section 3.3); and (ii) it visualises the empirical multivariate distribution for two of the five variables that is used in the Monte Carlo simulation (Section 3.4 and raised in Comment 24).
- To avoid any confusion for the reader, we have updated the caption of Figure 1 to cite the underlying data source, describe the multi-modal nature of the aircraft mass and nvPM distributions, and explain the changes in nvPM EI_n with altitude:
    - [Main text: Lines 233 – 238] "Figure 1: ~~The m~~**M**ultivariate distribution of aircraft mass and nvPM EI_n for one aircraft-engine group (light aircraft mass~~,~~ and nominal nvPM EI_n**, see Table 2**) at 32,000 feet (in blue) and 40,000 feet (in orange). **The underlying data is provided by the 2019 global aviation emissions inventory based on ADS-B (GAIA) (Teoh et al., 2024b). The multi-modal distribution of the aircraft mass and nvPM EI_n is due to the inclusion of two comparable aircraft engine families (Boeing 737 and Airbus A320 families) in the same group, each exhibiting distinct operating characteristics. The variations in nvPM EI_n with altitude results from changes in aircraft mass and air density, both of which influence the engine thrust settings and subsequently nvPM emissions (EASA, 2021).**"

24. *In addition, the use of Figure 1 in Section 3.4 is ambiguous. My understanding is that it is an example of a multivariate distribution, and that the Monte Carlo analysis relies on many similar figures. Is that correct? It would be good to clarify the role of Figure 1 in that section.*

- Thank you for highlighting this. To account for multi-collinearity between different aircraft performance parameters, the Monte Carlo simulation uses a five-dimensional empirical multivariate distribution constructed for each of the 12 aircraft-engine groups. Figure 1 illustrates the relationship between two of the five aircraft performance parameters (aircraft mass and nvPM EI_n) for one aircraft-engine group (light mass and nominal nvPM EI_n)
- To prevent any potential confusion for the reader, we have revised the text in Section 3.4 to make clear that a five-dimensional empirical multivariate distribution is used and to clarify the specific role of Figure 1:
    - [Main text: Lines 259 – 261] "~~For each aircraft-engine group, w~~**W**e account for ~~the~~ multi-collinearity **among** ~~between~~ different aircraft performance parameters (i.e., V_{TAS}, M, $\dot{m}_f$, η, and nvPM EI_n) by constructing a~~n~~ **five-dimensional** empirical multivariate distribution for each **aircraft-engine** group**.** ~~to sample the required aircraft performance parameters (~~Fig**ure**~~.~~ 1

illustrates an example of the relationship between two (*M* and nvPM EI_n) of these five variables~~)~~."

- [Main text: Lines 264 – 267] "Within each **set** of ~~these~~ 10 simulation runs, the aircraft performance parameters (i.e., V_{TAS}, ***M*** ~~aircraft mass~~, $\dot{m}_f$, η, and nvPM EI_n) at different altitudes are **sampled** ~~drawn~~ from the **five-dimensional** empirical multivariate distribution ~~(Fig. 1)~~ and α is sampled from a uniform distribution that ranges between 0° and 360°."

25. *Line 225: What is meant by "is set up"? Is that something you did for that section, or some built-in capability of the model? Some practical information would be useful here.*

- We have revised this sentence to make clear that the Monte Carlo simulation is a built-in capability of the grid-based CoCiP:
  - [Main text: Line 248] "The grid-based CoCiP **can perform** ~~is set up to run in~~ Monte Carlo simulations to **produce a range of $EF_{contrail}$ estimates for each grid cell** ~~explore the uncertainties related to model simplifications (i.e., aircraft-engine groups and the treatment of α) and meteorological forecasts~~."

26. *Line 234: Are 100 Monte-Carlo simulations enough to get robust uncertainties? That seems like a small number given the number of uncertain parameters and their uncertainty ranges.*

- The choice of 100 Monte Carlo simulation runs was primarily driven by computational resource constraints. As a sanity check, we plotted the running mean of $EF_{contrail}$ per flight distance against the number of Monte Carlo simulation runs for a specific time slice (03:00:00 on the 7th of January 2019, which is same time slice used to produce Fig. 9b). For the uncertainty parameters covered in this study (i.e., meteorology, aircraft performance, emissions, and treatment of the segment angle), the plot (below) indicates that 100 runs are sufficient for the $EF_{contrail}$ to converge:

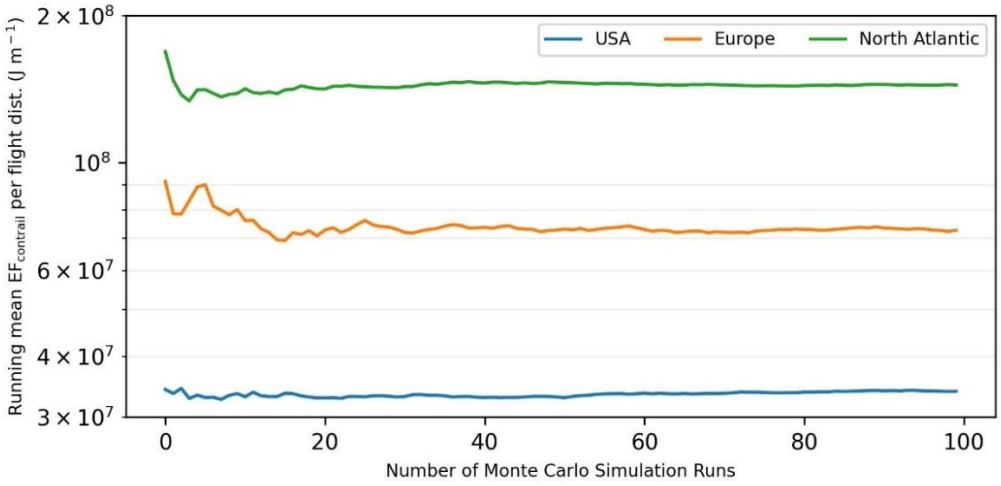

- Since the Monte Carlo simulation in this study serves as a proof of concept to demonstrate how uncertainties in contrail forecasts can be integrated into flight planning, we have not included further discussions on this topic in the revised manuscript, as it falls beyond the scope of this research.

- Nevertheless, we highlight a recent publication by Platt et al. (2024), which evaluates the impact of various uncertainty sources on $EF_{contrail}$ estimated using an earlier version of the grid-based CoCiP.
- To address this comment, we have revised the manuscript to emphasise that our Monte Carlo simulations are intended as a proof of concept. We also highlighted the different uncertainty sources and noted that these uncertainty sources will be incorporated in future releases of the grid-based CoCiP:
    - [Main text: Lines 248 – 257] "The grid-based CoCiP **can perform** ~~is set up to run in~~ Monte Carlo simulations to **produce a range of $EF_{contrail}$ estimates for each grid cell. Here, we utilize this capability to demonstrate how uncertainties in contrail forecasts can be integrated into flight planning (Section 5.3). We note that the uncertainties in the simulated $EF_{contrail}$ can arise from multiple independent sources, including meteorological inputs provided by NWP models, aircraft performance and emissions estimates, contrail model simplifications, the parametric RF model fitted to the libRadtran radiative transfer package, and potentially other unidentified factors (Low et al., 2024; Platt et al., 2024; Schumann et al., 2021; Teoh et al., 2020b, 2024a). While Platt et al. (2024) evaluates various uncertainty sources affecting $EF_{contrail}$ in an earlier implementation of the grid-based CoCiP, the Monte Carlo simulations in this study focuses only on** ~~explore the~~ uncertainties related to **meteorological inputs and the grid-based** model simplifications (i.e., aircraft-engine groups and ~~the~~ treatment of α) ~~and meteorological forecasts~~ **as a proof of concept**. **Future updates to the grid-based CoCiP will incorporate additional uncertainty sources to improve the model's robustness.**"
    - [Main text: Lines 497 – 500] "Here, we propose two strategies **as a proof of concept** to incorporate ~~these~~ **contrail forecast** uncertainties in the decision-making process of contrail mitigation~~, thereby~~**. Our goal of providing a range of $EF_{contrail}$ estimates is to** increase**ing** the probability of achieving a net climate benefit, and minimise**ing** the unintended consequences associated with increased fuel consumption and long-lived CO_2 emissions."

27. *Line 260: But to determine the proportion of flights that exert 80% of total annual energy forcing, the model needs to be able to simulate the whole distribution properly. Unless you take an approximated view of the percentile boundaries?*

- Thank you for raising this point. To address this, we have added a short description at the beginning of Section 3 to make clear that the percentile boundaries for $EF_{contrail}$ per flight distance, which are used by the grid-based CoCiP to define regions with strongly warming contrails, came from a historical global contrail simulation in 2019 using the trajectory-based CoCiP:
    - [Main text: Lines 154 – 163] "One way to address this limitation is to produce a 4D field of the $EF_{contrail}$ per flight distance flown, effectively identifying regions forecast to form persistent **and/or strongly** warming contrails. We achieve this by extending the trajectory-based CoCiP to a grid-based approach, where an infinitesimal contrail segment is: (i) initialized at each point in a 4D spatiotemporal domain; (ii) simulated until its end of life with a d*t* of 300 s

using the equations of the trajectory-based CoCiP; and (iii) has its cumulative climate forcing attributed back to the grid cell where it originally formed, with the model outputs taking the same form as traditional 4D NWP data. For (ii), Appendix A2 evaluates the sensitivity of d*t* on the simulated $EF_{contrail}$ and provides the rationale for selecting a d*t* of 300 s for the grid-based CoCiP. **Additionally, we note that the grid-based CoCiP defines regions with strongly warming contrails based on the 80th percentile (5 ×10^{8} J m^{-1}) and the 95th percentile (1.5 ×10^{9} J m^{-1}) of $EF_{contrail}$ per flight distance flown, both of which were derived from a 2019 global contrail simulation using the trajectory-based CoCiP (Teoh et al., 2024a).**"

28. *Lines 377-378: Is this statement an introduction to what follows? What is the consistency with Bier and Burkhardt (2022) and Gettleman et al. (2021)? Are you talking about qualitative or quantitative consistency?*

- Thank you for highlighting this. We have revised this sentence to clarify the variables being compared with earlier global contrail simulation studies and to set the context for the discussion to follow:
    - [Main text: Lines 409 – 414] "The grid-based CoCiP**'s prediction of persistent contrail occurrence and spatial trends in $EF_{contrail}$ are** generally ~~provides results that are~~ consistent with **earlier global contrail simulation studies** ~~prior research~~ (Bier and Burkhardt, 2022; Gettelman et al., 2021; Teoh et al., ~~2022a,~~ 2024a). **For example,** ~~T~~the absence of persistent contrails below 35,000 feet in the tropics (Fig. 6a and 6b) is primarily attributed to its higher relative ambient temperatures and tropopause height (Santer et al., 2003), while the lower relative $EF_{contrail}$ per flight distance at the subtropics (i.e., China, India, Middle East, and Australia, as shown in Fig. 6c) is associated with a lower persistent contrail formation due to the Hadley circulation (Teoh et al., 2024a)."

29. *Line 476: Are those findings based on the one-day case shown on Figure 9b? How generic are they?*

- We have revised this sentence to make clear that our findings are based on a visual examination of the $EF_{contrail}$ uncertainties at a specific point in time:
    - [Main text: Lines 505 – 506] "**A visual examination of** ~~Our analysis reveals three key features regarding~~ the uncertainties in the simulated $EF_{contrail}$ **at a specific point in time reveals three key features**: …"
- To determine if these findings are generally applicable, a different methodology beyond a visual evaluation would be needed to conduct a large-scale comparison of these uncertainty patterns at each time step.

30. *Line 477: Regions of lower uncertainties seem to be also located at the edges and in pockets.*

- As our findings are based on a visual examination (mentioned in Comment 29), we have made the following changes in the revised manuscript to reflect a more cautious interpretation of these findings:
    - [Main text: Lines 505 – 511] "**A visual examination of** ~~Our analysis reveals three key features regarding~~ the uncertainties in the simulated $EF_{contrail}$ **at a specific point in time reveals three key features**: (i) ~~uncertainties in the~~ $EF_{contrail}$ **uncertainties** are generally larger~~st~~ at the edges and localised pockets of ISSRs; (ii) the sign of $EF_{contrail}$ **tend to be more stable on a** ~~exhibit greater stability at the~~ synoptic ~~length~~ scale (i.e., ISSRs with horizontal coverages of ~1000 km); and (iii) persistent contrails formed at night and in winter~~time tend to exhibit~~ **are more likely to have a** lower relative uncertainty compared to those formed during daytime and in the summer (**i.e., Northern vs. Southern hemisphere, shown in** Fig. 9b). These results ~~also~~ suggest that contrail interventions may be more effective when implemented at a regional level rather than **targeting** individual flight**s as** ~~trajectories because the~~ contrail uncertainties **in** ~~at a~~ specific **locations** ~~space~~ and time may be lower than **in** other **areas** ~~regions~~."

31. *Line 771: How is the fuel cost of changing altitude calculated? Is that part of the performance model?*

- Thank you for highlighting this. We have revised the paragraph to make clear that the fuel cost of changing altitudes is provided by the Poll-Schumann (PS) aircraft performance model. We also note that the model accounts for factors such as the ambient wind conditions at different altitudes to estimate the fuel consumption:
    - [Main text: Lines 862 – 871] "Starting from the initial point of the horizontal grid and the lowest flight level, the algorithm iterates through each of the feasible grid points to determine the optimal Mach number (M_{opt}) for the given aircraft type and CI. The M_{opt} that minimizes the total cost of cruise at each flight segment is given by:

$$M_{\text{opt}} = \underset{M}{\text{argmin}} \left(\frac{\text{CI} + \Delta m(M)}{V_{\text{TAS}}} \right), \qquad \text{(A13)}$$

where **the** CI is ~~the chosen cost index (~~assumed to be 60 in this study~~)~~, $\Delta m(M)$ is the fuel burn over this flight segment for a given Mach number (M), and V_{TAS} is the aircraft true airspeed ~~which accounts for the ambient wind conditions~~. The fuel burn **for the original and alternative flight paths, which represent different cruise altitude options,** is computed using the Poll-Schumann (PS) aircraft performance model (Poll and Schumann, 2020, 2021, 2024)**. The estimated fuel burn accounts for various input parameters such as** ~~and requires~~ the aircraft type, ambient air temperature**, ambient wind conditions (which influence V_{TAS}),** and aircraft mass ~~as input parameters~~."

REFERENCES

Frömming, C., Grewe, V., Brinkop, S., Jöckel, P., Haslerud, A. S., Rosanka, S., Van Manen, J., and Matthes, S.: Influence of weather situation on non-CO2 aviation climate effects: The REACT4C climate change functions, Atmos Chem Phys, 21, 9151–9172, https://doi.org/10.5194/ACP-21-9151-2021, 2021.

Gaillot, T., Beauchet, S., Lorne, D., and Krim, L.: The impact of fossil jet fuel emissions at altitude on climate change: A life cycle assessment study of a long-haul flight at different time horizons, Atmos Environ, 311, 119983, https://doi.org/10.1016/J.ATMOSENV.2023.119983, 2023.

Gryspeerdt, E., Stettler, M. E. J., Teoh, R., Burkhardt, U., Delovski, T., Driver, O. G. A., and Painemal, D.: Operational differences lead to longer lifetimes of satellite detectable contrails from more fuel efficient aircraft, Environmental Research Letters, 19, 084059, https://doi.org/10.1088/1748-9326/AD5B78, 2024.

Jeßberger, P., Voigt, C., Schumann, U., Sölch, I., Schlager, H., Kaufmann, S., Petzold, A., Schäuble, D., and Gayet, J.-F.: Aircraft type influence on contrail properties, Atmos Chem Phys, 13, 11965–11984, https://doi.org/10.5194/acp-13-11965-2013, 2013.

Lokman, N.: MUAC Contrail Prevention Trial 2021, 2022.

Märkl, R. S., Voigt, C., Sauer, D., Dischl, R. K., Kaufmann, S., Harlaß, T., Hahn, V., Roiger, A., Weiß-Rehm, C., Burkhardt, U., Schumann, U., Marsing, A., Scheibe, M., Dörnbrack, A., Renard, C., Gauthier, M., Swann, P., Madden, P., Luff, D., Sallinen, R., Schripp, T., and Le Clercq, P.: Powering aircraft with 100 % sustainable aviation fuel reduces ice crystals in contrails, Atmos Chem Phys, 24, 3813–3837, https://doi.org/10.5194/ACP-24-3813-2024, 2024.

Platt, J., Shapiro, M., Engberg, Z., McCloskey, K., Geraedts, S., Sankar, T., Stettler, M. E. J., Teoh, R., Schumann, U., Rohs, S., Brand, E., and Van Arsdale, C.: The effect of uncertainty in humidity and model parameters on the prediction of contrail energy forcing, Environ Res Commun, https://doi.org/https://doi.org/10.1088/2515-7620/ad6ee5, 2024.

Rennert, K., Errickson, F., Prest, B. C., Rennels, L., Newell, R. G., Pizer, W., Kingdon, C., Wingenroth, J., Cooke, R., Parthum, B., Smith, D., Cromar, K., Diaz, D., Moore, F. C., Müller, U. K., Plevin, R. J., Raftery, A. E., Ševčíková, H., Sheets, H., Stock, J. H., Tan, T., Watson, M., Wong, T. E., and Anthoff, D.: Comprehensive evidence implies a higher social cost of CO2, Nature 2022 610:7933, 610, 687–692, https://doi.org/10.1038/s41586-022-05224-9, 2022.

Sausen, R., Hofer, S. M., Gierens, K. M., Bugliaro Goggia, L., Ehrmanntraut, R., Sitova, I., Walczak, K., Burridge-Diesing, A., Bowman, M., and Miller, N.: Can we successfully avoid persistent contrails by small altitude adjustments of flights in the real world?, Meteorologische Zeitschrift, https://doi.org/10.1127/metz/2023/1157, 2023.

Schumann, U., Mayer, B., Graf, K., and Mannstein, H.: A parametric radiative forcing model for contrail cirrus, J Appl Meteorol Climatol, 51, 1391–1406, https://doi.org/10.1175/JAMC-D-11-0242.1, 2012.

Teoh, R., Engberg, Z., Shapiro, M., Dray, L., and Stettler, M. E. J.: The high-resolution Global Aviation emissions Inventory based on ADS-B (GAIA) for 2019–2021, Atmos Chem Phys, 24, 725–744, https://doi.org/10.5194/ACP-24-725-2024, 2024.

Wolf, K., Bellouin, N., and Boucher, O.: Distribution and morphology of non-persistent contrail and persistent contrail formation areas in ERA5, Atmos Chem Phys, 24, 5009–5024, https://doi.org/10.5194/ACP-24-5009-2024, 2024.